Development of the first potential nonpeptidic positron emission tomography tracer for the imaging of CCR2 receptors

Wagner, S.; Moura Gatti, F.; Silva, D.G. de; Ortiz Zacarias, N.V.; Zweemer, A.J.M.; Hermann, S.; ... ; Junker, A.

Citation

Note: To cite this publication please use the final published version (if applicable).

Check for updates

Chemistry
Europe
European Chemical
Societies Publishing

VIP *Very Important Paper*

Development of the First Potential Nonpeptidic Positron Emission Tomography Tracer for the Imaging of CCR2 Receptors

Stefan Wagner+,[a] Fernando de Moura Gatti+,[b, i] Daniel G. Silva,[c] Natalia V. Ortiz Zacarias,[d] Annelien J. M. Zweemer,[d] Sven Hermann,[c] Monica De Maria,[e] Michael Koch,[f] Christina Weiss,[f] Dirk Schepmann,[b] Laura H. Heitman,[d] Nuska Tschammer,[g] Klaus Kopka,[h] and Anna Junker*[b, c]

Herein we report the design and synthesis of a series of highly selective CCR2 antagonists as ^{18}F-labeled PET tracers. The derivatives were evaluated extensively for their off-target profile at 48 different targets. The most potent and selective candidate was applied *in vivo* in a biodistribution study, demonstrating a promising profile for further preclinical development. This compound represents the first potential nonpeptidic PET tracer for the imaging of CCR2 receptors.

Introduction

The C—C chemokine receptor type 2 (CCR2) is a key player in the trafficking of lymphocytes and monocytes/macrophages leading to the development of various pathophysiological processes like inflammatory and autoimmune diseases,[1] tumor growth and metastasis formation.[2] CCR2 receptor is increasingly gaining attention in the field of positron emission tomography (PET) imaging as a promising diagnostic target for lung inflammation,[3] injured heart[4] or pancreatic ductal adenocarcinoma (phase 1; NCT03851237, 1R01CA235672-01, 201807099). So far only a peptidic ligand that binds to the first extracellular loop of the CCR2 receptor ECL1i was applied in PET imaging either as ^{64}Cu-DOTA-ECL1i or ^{68}Ga-DOTA-ECL1i

conjugate.[3–4] There are no small-molecule, nonpeptidic PET tracers for the imaging of CCR2 receptors reported thus far.

The CCR2 receptors share 71% sequence identity and an overlapping expression pattern with the C—C chemokine type 5 (CCR5) receptors.[5] The CCR5 receptor is expressed on a variety of cells and tissues such as monocytes, macrophages, T-lymphocytes, microglia, dendritic cells, the endothelium, and vascular smooth muscle. The CCR2 expression is more restricted to certain cell types such as monocytes, NK (natural killer) cells, and T lymphocytes.[6] Many potent CCR2 ligands demonstrate affinity to both receptors.[7] In the past, we have reported the design and synthesis of novel, selective as well as dual-targeting CCR2 and CCR5 receptor antagonists,[8] as well as the positive allosteric modulators (PAMs) for the CCR5 receptors.[9] Based on

[a] Dr. S. Wagner+
Department of Nuclear Medicine
University Hospital Münster
Albert-Schweitzer-Campus 1, Building A1
48149 Münster (Germany)

[b] Dr. F. de Moura Gatti,+ Dr. D. Schepmann, Dr. A. Junker
Institut für Pharmazeutische und Medizinische Chemie der Universität Münster
Corrensstraße 48, 48149 Münster (Germany)

[c] Dr. D. G. Silva, Dr. S. Hermann, Dr. A. Junker
European Institute for Molecular Imaging (EIMI)
Waldeyerstraße 15, 48149 Münster (Germany)
E-mail: anna.junker@wwu.de

[d] Dr. N. V. Ortiz Zacarias, Dr. A. J. M. Zweemer, Prof. Dr. L. H. Heitman
Leiden Academic Centre for Drug Research (LACDR)
Leiden University
Einsteinweg 55, 2333 CC Leiden (The Netherlands)

[e] M. De Maria
Department of Developmental Biology
Friedrich Alexander University
Staudtstraße 5, 91058 Erlangen (Germany)

[f] Dr. M. Koch, C. Weiss
Bayer AG, Research & Development
Lead Discovery Wuppertal
Aprather Weg 18a, Gebäude 456
42096 Wuppertal (Germany)

[g] Dr. N. Tschammer
Department of Chemistry and Pharmacy
Emil Fischer Center
Friedrich Alexander University Erlangen–Nürnberg
Schuhstraße 19, 91052 Erlangen (Germany)

[h] Prof. Dr. K. Kopka
Helmholtz-Zentrum Dresden-Rossendorf
Institut für Radiopharmazeutische Krebsforschung
Bautzner Landstraße 400
01328 Dresden (Germany)
and
Faculty of Chemistry and Food Chemistry
Technische Universität Dresden
01062 Dresden (Germany)

[i] Dr. F. de Moura Gatti+
Faculdade de Ciências Farmacêuticas
Universidade de São Paulo
Av. Prof. Lineu Prestes, 580
CEP 05508-900, São Paulo, SP (Brazil)

[+] These authors contributed equally to this work.

this work we envisaged to evaluate fluorine-18 radiolabeled CCR2 targeting ligands as PET radiotracers for molecular imaging of inflammation and cancer.
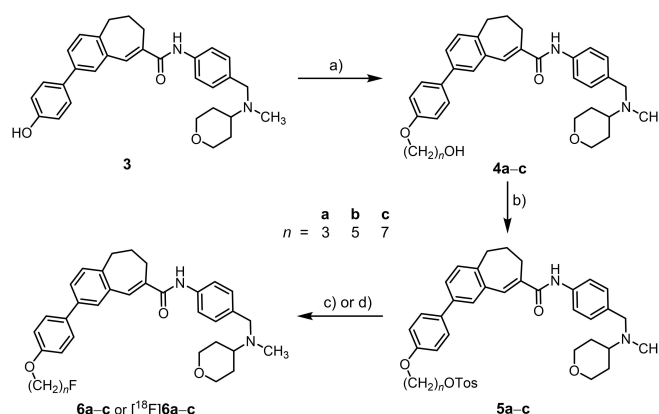
Our previous structure–activity and structure–affinity studies of novel CCR2 and CCR5 receptors targeting compounds derived from TAK-779 (**1**) revealed a first strategy for the introduction of high CCR2 receptor selectivity. While TAK-779 (**1**) is more or less equipotent at CCR2 and CCR5 receptors introduction of a bulky isopropoxy residue at the 6-position of a pyridine ring as seen in compound **2** (Figure 1) yielded different properties of binding to the active site residues within the CCR2 and CCR5 receptors, leading to higher CCR2 selectivity (Table 1, IC_{50} ([^{125}I]CCL2) $= 19$ nM vs. IC_{50} ([^{3}H]TAK-779) $= 468$ nM). Other pyridine derivatives were inactive.[8a]

Results and Discussion

Following the idea of addressing different electrostatic properties by the isopropoxy derivative **2**, a series of CCR2 selective antagonists **6a–c** bearing a flexible ω-fluoroalkoxy side chain was developed. The phenol derivative **3** served as a starting structure for the introduction of the alkoxy side chain. As the influence of the chain length on the CCR2 and CCR5 receptor activity/affinity should be examined, propyloxy (**4a**, $n = 3$),

Scheme 1. Synthesis of ω-fluoroalkyl derivatives **6a–c**. a) ω-bromoalkan-1-ol (1.1 equiv.), K_2CO_3 (2 equiv.), DMF, 60 °C, 12 h, 70–84%; b) DMAP (0.25 equiv.), Et_3N (4.65 equiv.), 4-toluenesulfonyl chloride (2 equiv.), −25 °C (0.5 h), then RT, 20 h, 74–90%; c) Bu_4NF (1 M in THF, 20 equiv.), THF, RT, 12 h, 73–84%; d) $K(K_{2.2.2})[^{18}F]F$, K_2CO_3, DMSO, 100 °C, 20 min.

pentyloxy (**4b**, $n = 5$) and heptyloxy (**4a**, $n = 7$) side chains were considered. The high acidity of the phenol **3** allows deprotonation with weak bases without affecting the primary alcohol of the ω-halogenalkanols used. The reactivity of the ω-halogen-alkanols is dependent on the halogen leaving group (I > Br > Cl). However, the reaction with 3-iodopropan-1-ol led to dialkylation of **3** (second alkyl group attached to the tertiary amine). Because we assumed that the dialkylation was due to the high reactivity of 3-iodopropan-1-ol, 3-bromopropan-1-ol with reduced reactivity was employed. Reaction of **3** with 3-bromopropan-1-ol and K_2CO_3 in DMF afforded selectively **4a** in 84% yield. The homologous alcohols **4b** and **4c** were prepared analogously by alkylation of phenol **3** with 5-bromopentan-1-ol and 7-bromoheptan-1-ol, respectively (Scheme 1). The compounds **5a–c** served as precursors for the development of fluorinated PET ligands [^{18}F]**6a–c**. The introduction of an ^{18}F-atom into the molecule requires a good leaving group. Therefore, the primary alcohols **4a–c** were converted into the tosylates **5a–c**. The reaction of the alcohols **4a–c** with tosyl chloride and 4-dimethylaminopyridine (DMAP, *Steglich* catalyst) provided the tosylates **5a–c**.[9] The *in vitro* receptor activities and affinities of the ^{18}F-labeled PET tracers cannot be recorded

Figure 1. TAK-779 (**1**) and compound **2**.

Table 1. CCR2 and CCR5 activities and affinities of TAK-779 (**1**), the reference compound **2**, the alcohols **3**, **4a–c** and fluorinated ligands **6a–c**.

Cmpd.	CCR2 $IC_{50} \pm$ SEM [nM]		Ca^{2+} flux, hCCR2	β-Arrestin, mCCR2	CCR5 [^{3}H]TAK-779 $IC_{50} \pm$ SEM [nM]	β Arrestin, hCCR5, CCL5-mediated K_b [nM]	cAMP BRET, CCL5-mediated K_b [nM]	cAMP BRET, CCL4-mediated K_b [nM]
	[^{125}I]CCL2	[^{3}H]INCB						
TAK-779 (**1**)	2.0 ± 0.7[a]	50 ± 5[a]	0.95[a]	23[a]	8.8 ± 1.7^a	12 ± 1.2	65.5	7.5
2	19 ± 4.2[a]	–	2.7[a]	90[a]	468^a	–	–	–
3	35%[b]	–	82	1360	1500	–	–	–
4a	199	51%[b]	45	783	970	–	–	–
4b	326	53%[b]	10	117	3100	–	–	–
4c	83	56%[b]	1.1	54	2300	–	–	–
6a	48%[b]	118 ± 20	130	1110	2700	684 ± 219	2300	551
6b	14 ± 7	609 ± 188	0.76	40	2000	529 ± 142	580	65.4
6c	93 ± 8	494 ± 38	1.1	17	3600	378 ± 114	288	27.1

All experiments were performed in at least triplicate ($n = 3$). [a] See ref. [8a]. [b] % inhibition at a test compound concentration of 1 μM.

ChemMedChem

Full Papers
doi.org/10.1002/cmdc.202000728

**Chemistry
Europe**
European Chemical
Societies Publishing

directly with the radiolabeled ligands due to the small amount and the short physical half-life of the labeled compounds. Therefore, the in vitro activities and affinities to the CCR2 and other receptors/targets were determined using the non-radio-active ^{19}F-labeled analogues. The synthesis of the non-radio-active ^{19}F counterparts **6a–c** can be performed by direct fluorination of the alcohols **4a–c** or by the introduction of an appropriate leaving group and subsequent S_N2 substitution. Tetrabutylammonium fluoride (TBAF) is a common fluorinating reagent. The bulky tetraalkylammonium counterion reduces the ionic bond strength and generates a "naked" fluoride ion with a good solubility in organic solvents.[10] As the tosylates **5a–c** were already prepared for the radiolabeling reaction, they were also employed for the fluorination with TBAF. Tosylates **5a–c** were reacted with TBAF in THF, which afforded the pure fluoro derivatives **6a–c** in 73–84% yield (Scheme 1).

The compounds were evaluated for their in vitro CCR2 activities and affinities as well as their selectivity towards CCR5 receptors in functional as well as in binding assays. The hydroxyalkoxy derivatives **4a–c** display very low CCR2 and CCR5 receptor affinities and moderate to high CCR2 receptor potencies (Table 1). The heptyloxy derivative with a primary alcohol at the end (**4c**) shows the highest CCR2 affinity/activity (IC$_{50}$([^{125}I]CCL2) = 83 nM, IC$_{50}$ (Ca^{2+}-flux, hCCR2) = 1.1 nM, IC$_{50}$ (β-arrestin, mCCR2) = 54 nM).

However, the fluoroalkoxy derivatives **6a–c** do not follow the same trend in their SAR. The pentyloxy compound **6b** displays the highest CCR2 binding in the [^{125}I]CCL2 assay with an IC$_{50}$-value of 14 nM and the highest CCR2 activity in the Ca^{2+}-flux assay using the human CCR2 receptor, indicating an IC$_{50}$-value of 0.76 nM. Furthermore, **6b** is highly selective against CCR5 receptors (IC$_{50}$ (CCR5; [^{3}H]TAK-779) = 2000 nM). The fluoroalkoxy derivatives **6a–c** show a probe-dependent CCR5 activity when compared to TAK-779; whereas TAK-779 (**1**) binding affects CCL5- as well as CCL4-dependent CCR5 receptor activity. The fluoroalkoxy derivatives **6b** and **6c** display only high activity in the cAMP-BRET CCL4-mediated assay with K$_b$ values of 65.4 and 27.1 nM, respectively. Only moderate activity is seen in β-arrestin and cAMP BRET CCL5-mediated CCR5 assays, indicating a different binding mode at the CCR5 receptors as compared with that of TAK-779 (**1**).

Moreover, the fluoroalkoxy derivatives **6a–c** were screened in the in-house σ$_1$, σ$_2$ assays and in a panel of 45 different targets (hERG, 5-HT$_{1A}$, 5-HT$_{1B}$, 5-HT$_{1D}$, 5-ht$_{1e}$, 5-HT$_{2A}$, 5-HT$_{2B}$, 5-HT$_{2C}$, 5-HT3, 5-HT$_{5a}$, 5-HT$_6$, 5-HT$_7$, D$_{1-5}$, SERT, NET, DAT, MOR, KOR, DOR, GABA$_A$, H$_{1-4}$, α$_{1A}$, α$_{1B}$, α$_{2A}$, α$_{2B}$, α$_{2C}$, α$_{1D}$, β$_{1-3}$, M$_{1-5}$, BZP Rat brain site, PBR) within the NIMH Psychoactive Drug Screen-
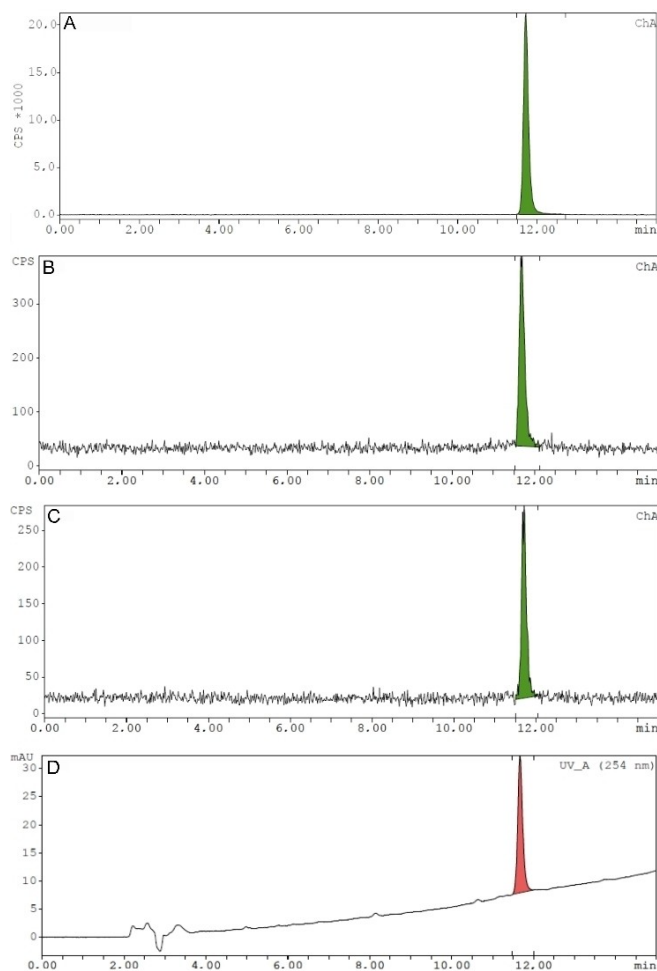
ing Program for their off-target affinity/activity. In Table 2, the data for detectable (< 10 μM) off-target affinity/activity of compounds **6a–c** is given. Hereby, the fluoropentoxy derivative **6b** displayed the highest selectivity profile within the series. Compound **6b** showed moderate affinity in the radioligand binding assays for σ$_1$ (K$_i$ ([^{3}H]-(+)-pentazocine) = 0.32 μM) and very low affinity to α$_{2B}$ receptors (K$_i$ ([^{3}H]Rauwolscine) = 6.81 μM). The inhibition of the hERG channel (Kv$_{11.1}$ potassium ion channel, KCNH2) is widely regarded as the predominant cause of drug-induced QT prolongation. The moderate hERG activity and, therefore, potential cardiotoxicity of compound **6b** of 1.72 μM in the FluxOR assay would represent a considerable limitation to a drug development program. However, diagnostic PET tracers are applied in extremely low concentrations; therefore, not reaching the effective concentration required for cardiotoxicity. Taken together, the fluoropentoxy derivative **6b** displayed high CCR2 affinity/activity combined with a favorable off-target selectivity profile and was therefore chosen as a promising candidate for in vivo evaluation as a potential PET tracer.

PET measurements can be performed with different radionuclides such as ^{11}C, ^{13}N, ^{15}O and ^{18}F. ^{13}N and ^{15}O are very limited due to their short physical half-life (< 10 min) and are mostly used for the imaging of perfusion processes.[11] [^{18}F]fluoride offers several advantages over [^{11}C]carbon, such as longer physical half-life (110 vs. 20 min), maximal β$^+$-particle energy of 650 keV vs. 960 keV, and higher quality images with higher spatial resolution in PET measurements.[11–12] In our efforts to develop an ^{18}F-labeled CCR2 receptor PET ligand, we selected compounds **6a–c** for radiolabeling and subsequently compound **6b** for the first evaluation in adult C57Bl/6 mice. Besides the high CCR2 receptor affinity and high selectivity over CCR5 and other biological targets, compounds **6a–c** offered the ability to be labeled in an one step nucleophilic substitution (S$_N$2-type) reaction of the tosyloxy moiety of **5a–c** with [^{18}F] fluoride. Ligands [^{18}F]**6a–c** were prepared by direct nucleophilic replacement of the tosyloxy moiety with [^{18}F]fluoride in a lead-

Table 3. Results of the radiosynthesis of compounds [^{18}F]**6a–c**.

Cmpd.	Synthesis time [min]	A$_m$ [GBq/μmol]	RCY [%] (decay-corrected)
[^{18}F]**6a**	94 ± 13	4–70	40 ± 3[a]
[^{18}F]**6b**	113 ± 27	3–31	28 ± 5[b]
[^{18}F]**6c**	91 ± 10	5–54	25 ± 6[c]

[a] $n=5$, [b] $n=9$, [c] $n=6$.

Table 2. Off-target affinities/activities of fluorinated ligands **6a–c**.

Cmpd.	σ$_1$ K$_i$ [μM]	σ$_2$ K$_i$ [μM]	α$_{2A}$ K$_i$ [μM]	α$_{2B}$ K$_i$ [μM]	M$_3$ K$_i$ [μM]	5-HT$_{2C}$ K$_i$ [μM]	5-HT$_{5A}$ K$_i$ [μM]	hERG EC$_{50}$ [μM]
6a	1.0	0.74	–	1.2	–	1.02	5.01	2.29 ± 0.31
6b	0.32	7%[a]	–	6.81	–	–	–	1.72 ± 0.092
6c	14%[a]	17%[a]	6.27	–	5.22	–	–	0.671 ± 0.220

Assays: K$_i$ values ± SEM from three independent experiments. [a] % inhibition at a test compound's concentration of 10 μM. Radioligands used for receptor binding studies were as follows: σ$_1$: [^{3}H]-(+)-pentazocine, σ$_2$: [^{3}H]ditolylguanidine, α$_{2A}$ and α$_{2B}$: [^{3}H]rauwolscine, M3: [^{3}H]QNB, 5-HT$_{2C}$: [^{3}H]mesulergine, 5-HT5A: [^{3}H]LSD, functional assays: FluxOR assay hERG: cisapride.

ChemMedChem

Full Papers
doi.org/10.1002/cmdc.202000728

Chemistry
Europe
European Chemical
Societies Publishing

Figure 2. Radio-HPLC chromatograms of A) a typical quality control (QC) of a produced [^{18}F]**6b** batch and of the *in vitro* stability of [^{18}F]**6b** after incubation in mouse blood serum at 37 °C after B) 10 min or C) 90 min and D) HPLC chromatogram (UV channel, l = 254 nm) of non-radioactive counterpart **6b**, measured at analytical HPLC-system **B**, method **B**.
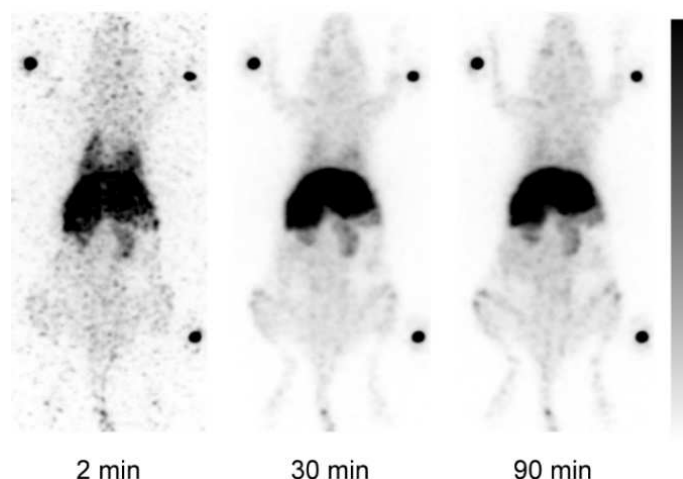

Figure 3. Quantitative analysis of radioactivity distribution in adult C57Bl/6 (n = 6) after intravenous injection of [^{18}F]**6b**. In vivo time–activity concentration curves a) and b) illustrate tracer distribution over time in blood (×), liver (△), gallbladder (▲), kidney (○), bladder (•), brain (·), lung (◆), spleen (◦), myocardium (·), and muscle (◦). In vivo data was complemented by subsequent ex vivo gamma counter analysis c). Results are expressed as mean + S.D. %ID is the percentage of injected dose.

shielded computer-controlled TRACERLab Fx$_{FDG}$ radiosynthesizer. In trial experiments, reaction of **5b** with [^{18}F]fluoride in DMSO gave a higher radiochemical yield (RCY) of [^{18}F]**6b** (30%) than in acetonitrile (5.5%). Compounds [^{18}F]**6a**–**c** were purified by semipreparative reversed-phase radio-HPLC in high radiochemical purities (> 99%). No residual precursors **5a**–**c** or other chemical impurities were detected in the formulated radioligand solution by analytical radio-HPLC. The molar activity (A_m) of the radioligands, when finally formulated for intravenous injection, the RCY and the synthesis times are given in Table 3. Furthermore, the partition coefficient log$D$ was experimentally determined for the radiolabeled compounds [^{18}F]**6a**–**c** at pH of 7.4. Compound [^{18}F]**6b** is the most lipophilic derivative of the series with a log$D$ (exp.) of 1.94 ± 0.26 (n = 5, calculated log$D$ value, c log$D$, of 7.00, was calculated by ACD/Chemsketch version ACD/Labs 6.00). For [^{18}F]**6a** a log$D$ (exp.) of 1.63 ± 0.17 (n = 5, c log$D$ = 6.17) and for [^{18}F]**6c** a log$D$ (exp.) of 1.69 ± 0.16 (n = 5, c log$D$ = 8.06) was determined. An *in vitro* stability study was carried out for all three radiolabeled compounds [^{18}F]**6a**–**c**

using mouse and human blood serum. During incubation for up to 90 min at 37 °C [^{18}F]**6a**, [^{18}F]**6b** and [^{18}F]**6c** possessed a high stability in both sera. Figure 2 shows exemplarily the data of [^{18}F]**6b** in mouse blood serum. Only the parent compound [^{18}F]**6b** was detected by radio-HPLC and no significant radio-metabolites or decomposition products could be observed. The behavior of [^{18}F]**6a** and [^{18}F]**6c** is the same (data not shown). Due to its high potency and binding affinity to the CCR2

ChemMedChem

Full Papers
doi.org/10.1002/cmdc.202000728

Chemistry Europe
European Chemical
Societies Publishing

Figure 4. Representative PET image data (maximum intensity projections, ventral view) of the *in vivo* biodistribution of [^{18}F]**6b** after intravenous injection in an adult female C57Bl/6 mouse.

receptor and its favorable off-target selectivity profile, the fluoropentyloxy derivative [^{18}F]**6b** was selected for the biodistribution studies.

Biodistribution of [^{18}F]6b in healthy adult C57Bl/6 mice

The radioactivity distribution of [^{18}F]**6b** was measured in adult C57Bl/6 mice *in vivo* over 90 minutes by PET/CT. PET images reveal fast and significant accumulation of radioactivity in the liver already in the first minutes after tracer injection that persists until the end of the study (Figure 4). A few minutes post-injection intermediate radioactivity levels were found in the lung, the spleen and the kidneys. Over the course of 90 minutes, the radioactivity concentration in the lungs decreased while the signal in the spleen and the kidneys remained at the same level. Image data do not show the elimination of the tracer and/or its metabolites in the urine. We observed a very slow and only marginally increase of radioactivity in the bones as a sensitive indicator of *in vivo* defluorination of the [^{18}F] labeled tracer, which demonstrated the expected stability of the fluoropentyl group against *in vivo* defluorination. Quantitative analysis by *in vivo* time–activity concentration curves and *ex vivo* gamma counting confirmed the visual impressions (Figure 3). The highly CCR2 selective radioligand [^{18}F]**6b** demonstrated favorable properties as a new diagnostic tool for PET to elucidate the changes in the distribution and density of CCR2 receptors, revealing their role in the development and pathobiology of inflammation or cancer.

Conclusion

Previously uncovered structure–activity/affinity relationships at CCR2 and CCR5 led the way to the development of highly potent and selective CCR2 receptor antagonists **4a–c** and **6a–c**, which were further converted into potential ^{18}F-labeled PET

tracer [^{18}F]**6a–c**. Compounds **6a–c** were excessively evaluated for their CCR2 activity/affinity and their off-target selectivity profile at CCR5 receptors and 47 other biological targets (GPCR, ion channels, transporters). The radiolabeled derivatives [^{18}F]**6a–c** were prepared in high purity ($>$99%) and high RCY (40–25%). Their log$D$, murine and human serum plasma stability was determined. The most potent and selective candidate [^{18}F]**6b** was evaluated *in vivo* in a biodistribution study. Thus displaying a promising profile for further preclinical development.

Experimental Section

Complete protocols for both chemical syntheses and biological methods together with characterization data are presented in the Supporting Information.

Author Contributions

The manuscript was written through the contributions of all authors. All authors have given approval to the final version of the manuscript. A.J. planned and synthesized all compounds. F.M.G. synthesized the precursor 5b in large scale. S.W., A.J. and D.G.S. performed the radiolabeling. Biological assays were performed by D.S., L.H., N.V.O.Z., A.Z., M.M., N.T., M.K. and C.W. The imaging experiments were performed by S.H.

Acknowledgements

Conflict of Interest

The authors declare no conflict of interest.

[1] a) G. Bajpai, A. Bredemeyer, W. Li, K. Zaitsev, L. Koenig Andrew, I. Lokshina, J. Mohan, B. Ivey, H.-M. Hsiao, C. Weinheimer, A. Kovacs, S. Epelman, M. Artyomov, D. Kreisel, J. Lavine Kory, *Circulation Res.* **2019**, *124*, 263–278; b) S. Bose, J. Cho, *Arch. Pharm. Res.* **2013**, *36*, 1039–1050.

[2] M. Feria, F. Díaz-González, *Expert Opin. Ther. Pat.* **2006**, *16*, 49–57.

[3] Y. Liu, S. P. Gunsten, D. H. Sultan, H. P. Luehmann, Y. Zhao, T. S. Blackwell, Z. Bollermann-Nowlis, J.-H. Pan, D. E. Byers, J. J. Atkinson, D. Kreisel, M. J. Holtzman, R. J. Gropler, C. Combadiere, S. L. Brody, *Radiology* **2017**, *283*, 758–768.

[4] G. S. Heo, B. Kopecky, D. Sultan, G. Feng, G. Bajpai, X. Zhang, H. Luehmann, L. Detering, K. Lavine, Y. Liu, *J. Nucl. Med.* **2019**, *60*, 98.

[5] T. A. Berkhout, H. M. Sarau, K. Moores, J. R. White, N. Elshourbagy, E. Appelbaum, R. J. Reape, M. Brawner, J. Makwana, J. J. Foley, D. B. Schmidt, C. Imburgia, D. McNulty, J. Matthews, K. O'Donnell, D. O'Shannessy, M. Scott, P. H. Groot, C. Macphee, *J. Biol. Chem.* **1997**, *272*, 16404–16413.

[6] a) C. Combadiere, S. K. Ahuja, H. L. Tiffany, P. M. Murphy, *J. Leukocyte Biol.* **1996**, *60*, 147–152; b) M. Samson, O. Labbe, C. Mollereau, G. Vassart, M. Parmentier, *Biochemistry* **1996**, *35*, 3362–3367.

[7] L. Fantuzzi, M. Tagliamonte, M. C. Gauzzi, L. Lopalco, *Cell. Mol. Life Sci.* **2019**, *76*, 4869–4886.

[8] a) A. Junker, A. K. Kokornaczyk, A. J. M. Zweemer, B. Frehland, D. Schepmann, J. Yamaguchi, K. Itami, A. Faust, S. Hermann, S. Wagner, M. Schafers, M. Koch, C. Weiss, L. H. Heitman, K. Kopka, B. Wunsch, *Org. Biomol. Chem.* **2015**, *13*, 2407–2422; b) A. K. Strunz, A. J. M. Zweemer, C. Weiss, D. Schepmann, A. Junker, L. H. Heitman, M. Koch, B. Wünsch, *Bioorg. Med. Chem.* **2015**, *23*, 4034–4049.

[9] S. Thum, A. K. Kokornaczyk, T. Seki, M. De Maria, N. V. Ortiz Zacarias, H. de Vries, C. Weiss, M. Koch, D. Schepmann, M. Kitamura, N. Tschammer, L. H. Heitman, A. Junker, B. Wünsch, *Eur. J. Med. Chem.* **2017**, *135*, 401–413.

[10] D. W. Kim, H.-J. Jeong, S. T. Lim, M.-H. Sohn, *Angew. Chem. Int. Ed.* **2008**, *47*, 8404–8406; *Angew. Chem.* **2008**, *120*, 8532–8534.

[11] M. Bruehlmeier, U. Roelcke, P. A. Schubiger, S. M. Ametamey, *J. Nucl. Med.* **2004**, *45*, 1851–1859.

[12] P. W. Miller, N. J. Long, R. Vilar, A. D. Gee, *Angew. Chem. Int. Ed.* **2008**, *47*, 8998–9033; *Angew. Chem.* **2008**, *120*, 9136–9172.